Plant Molecular Biology Reporter (2023) 41:675–689
https://doi.org/10.1007/s11105-023-01392-8

RESEARCH

An Arabidopsis Linker Histone-Like Protein Harbours a Domain with Adenylyl Cyclase Activity

Oziniel Ruzvidzo[1] · **Patience Chatukuta**[1]

Received: 28 February 2023 / Accepted: 30 May 2023 / Published online: 27 June 2023

Abstract

Adenylyl cyclase (AC) is an enzyme that catalyses the formation of the second messenger molecule, 3′,5′-cyclic adenosine monophosphate (cAMP) from 5′-adenosine triphosphate (ATP). cAMP, in turn, regulates key physiological processes such as cell division, growth, reproduction, development and response to stress. However, while cAMP is increasingly becoming an important signalling molecule in higher plants, the identification of plant ACs has somewhat remained so slow. In *Arabidopsis thaliana* alone, only twelve ACs have so far been identified, yet considering the number and diverse nature of processes known to be cAMP-dependent in this plant, these identified ACs are still very much few to account for that. Notably, an additional protein in this plant, termed linker histone-like (AtLHL) protein (encoded by the At3g18035 gene), is annotated to be an AC as result of it containing a putative centre identical to the one commonly found in the other twelve previously confirmed Arabidopsis ACs. In addition, AtLHL is mostly involved in a number of key cellular processes such as heterochromatin formation, DNA repair, apoptosis, embryogenesis, reproduction and disease resistance that are all modulated by cAMP, yet AtLHL still remains unconfirmed as an AC. As a result, we targeted this protein in this study to determine if it is indeed an AC. To begin with, we used computational analysis to assess the 3-dimensional (3D) structure of AtLHL and found that its AC centre is solvent-exposed, amenable to the unhindered access of ATP as a substrate for catalysis. Next, we cloned, partially expressed and affinity purified a truncated version of this protein ($AtLHL^{301-480}$), followed by assessment of its probable AC activity. Through enzyme immunoassay and mass spectrometry, we showed that the recombinant $AtLHL^{301-480}$ protein can generate cAMP from ATP in vitro in a manganese-dependent manner that is enhanced by calcium and hydrogen carbonate. In addition, we also showed that the recombinant $AtLHL^{301-480}$ protein can complement AC-deficiency (*cya*A mutation) in SP850 cells when expressed in this mutant *Escherichia coli* host strain. We then used electrochemistry to evaluate the molecular interaction of $AtLHL^{301-480}$ with its co-factors and modulators during catalysis and activation, respectively, and found that the protein does this physically. This observation then prompted us to specifically search for the presence (and possibly frequency) of calcium-binding sites within the AtLHL protein. Through in silico analysis and bioinformatic studies, a single binding site in form of a 16-residue calmodulin-binding sequence was predicted. Lastly, we then evaluated the reaction kinetics of $AtLHL^{301-480}$ and determined that the protein has a K_m constant of 0.7 mM and a V_{max} constant of 9.2 fmol/min/µg protein. All in all, our study provided adequate evidence in a multi-faceted manner that LHL from *A. thaliana* is a bona fide AC, whose activity might be involved in control and molecular regulation of the various functions of this protein in this plant.

Keywords *Arabidopsis thaliana* · Linker histone protein · Adenylyl cyclase · cAMP

Key Message
This study provides practical evidence that a linker histone-like protein from *Arabidopsis thaliana* (AtLHL) is a bona fide adenylyl cyclase (AC) capable of generating the second messenger cAMP from ATP, thus linking the protein to signalling and providing foundation for further studies to possibly shed more light onto its probable mode of action and/or functional significance in plants, particularly crops.

Extended author information available on the last page of the article

Introduction

Linker histone (LH) protein or H1 is one of the five main histone protein families that are components of chromatin in eukaryotic cells (Luger et al. 1997; Davey et al. 2002; Alberts et al. 2002; Albert et al. 2007). Other protein families are H2A, H2B, H3 and H4, which exist in pairs (octamer) together with DNA wound around them, forming

a nucleosome (Alberts et al. 2002; Albert 2007; Dekker 2008; Naumova et al. 2013). This nucleosome component or nucleosome 'bead' is actually the basic unit of chromatin or simply the first level of chromatin compaction (Alberts et al. 2002; Albert et al. 2007). Unlike the other histone proteins, LH does not really make up the nucleosome 'bead'; instead, it positions itself on top of the structure, keeping in place the DNA that is wrapped around the nucleosome. In terms of protein composition in the structure, LH constitutes half the amount of the other individual four histone proteins, which principally contribute two molecules each to the nucleosome 'bead'. In addition to binding to the nucleosome, LH binds to the 'linker DNA' (approximately 20–80 nucleotides in length) region between nucleosomes, helping stabilize the zig-zagged 30-nm chromatin fibre (Jeon and Berezney 1995).

While most of the LH protein in the nucleus is bound to chromatin, LH molecules shuttle between chromatin regions at a fairly high rate (Misteli et al. 2000; Chen et al. 2006). It is absolutely difficult to understand how such a dynamic protein could be a structural component of chromatin. Apparently, it has been suggested that the steady-state equilibrium within the nucleus still strongly favours association between LH and chromatin. This then means that despite its dynamics, the vast majority of this protein, at any given time point, is chromatin-bound (Bustin et al. 2005). LH compacts and stabilizes DNA under force and during chromatin assembly. This thus suggests that the dynamic binding of this protein may provide protection for DNA in situations where nucleosomes need to be removed (Xiao et al. 2012). Another important feature of the LH protein family is its heterogeneity. Multiple LH sub-types exist and are expressed in organisms as diverse as plants and humans, with eleven of them, namely, H1.0, H1.1, H1.2, H1.3, H1.4, H1.5, H1t, H1T2, H100, H1LS1 and H1X, found in mammals (Parseghian et al. 1994).

Like the other histone proteins, the LH family is extensively post-translationally modified. Such post-translational modifications (PTMs) include serine and threonine phosphorylation, lysine acetylation, lysine methylation, ADP ribosylation, ubiquitination, formylation, PARylation and O-glycosylation (Poirier et al. 1982; Garcia et al. 2004; Villar-Garea and Imhof 2006; Jiang et al. 2007; Wiśniewski et al. 2007, 2008; Deterding et al. 2008; Snijders et al. 2008; Lu et al. 2009; Bonet-Costa et al. 2012; Kim et al. 2015; Sarg et al. 2015). These PTMs are involved in the coordination of a variety of processes in the cell, although such involvement is somewhat less studied in LH compared to the other histone proteins. Nonetheless, LH phosphorylation and O-glycosylation have been shown to play a key role in chromatin compaction and remodelling; heterochromatin formation; DNA replication, transcription and repair; apoptosis; microtubule organization; and protein expression and PTM (Thoma and Koller 1977; Thoma et al. 1979; van Holde and Zlatanova 1996; Calikowski et al. 2000; Kim et al. 2012; Harshman et al. 2013). In addition, LH is also involved in other key cellular and biological processes (Hergeth and Schneider 2015) such as embryogenesis, where it controls the expression of pluripotency genes (Tanaka et al. 2003); reproduction, where it controls the differentiation of sperm cells (Martianov et al. 2005); and disease resistance, where it regulates the innate immune and stress response genes (Studencka et al. 2011).

However, despite the fact that all these processes listed above are typically mediated by the second messenger molecule 3′,5′-cyclic adenosine monophosphate (cAMP) generated by adenylyl cyclases (ACs) (Ito et al. 2014; Kasahara et al. 2016; Vaz Diaz et al. 2019), no histone protein to date, including LH, has been shown to possess AC activity. The only information available so far is the existence of a LH-like or HON4 protein (encoded by the At3g18035 gene) in *Arabidopsis thaliana* (AtLHL), annotated to be an AC (Gehring 2010). Therefore, focusing on these premises, we targeted AtLHL in this study to determine if it is an AC and perhaps to be able to at least better contextualize its currently known functions.

Materials and Methods

At3g18035 Gene Sequence and AtLHL Protein Sequence Analysis

Complete copy DNA (cDNA) and amino acid sequences of At3g18035 and AtLHL respectively, were retrieved from The Arabidopsis Information Resource (TAIR) (https://www.arabidopsis.org/), followed by analysis of the AtLHL sequence for presence of the AC catalytic centre (Gehring 2010) using the PROSITE database located within the Expert Protein Analysis System (ExPASy) proteomics server (https://www.expasy.org/). In addition, both the presence and location of the AC centre in AtLHL were further confirmed by ACPred, available at http://gcpred.com/acpred/ (Xu et al. 2018).

Computational Analysis of the AtLHL Protein

A 3-dimensional (3D) model of the AtLHL protein was constructed by artificial intelligence using its AlphaFOLD beta version with low predicted error and very high confidence (pLDDT > 90) (Varadi et al. 2022). This software uses a neural network-based model of artificial intelligence to predict protein structures from their amino acid sequences at an atomic level of accuracy. It first aligns the amino acid sequence input with sequences of known structures for pairwise representation. The representation is then used to produce atomic coordinates for each residue, thus predicting the necessary rotation and then assembling a structured chain of amino acid residues. Its developers freely provide the source

code for access to trained modellers and a script for predicting structures of novel input sequences (Varadi et al. 2022). In our case, the full-length amino acid sequence of AtLHL was submitted to the AlphaFOLD database followed by downloading of the model with the highest quality (based on C-scores). The downloaded model was then visualized and analysed using UCSF ChimeraX next-generation molecular visualization program (v.1.10.1.) (Pettersen et al. 2021). SeeSAR 3D (v.12.0.1) desktop modelling platform was next used to perform docking of ATP (PubChem ID: 5957) to the AC centre of the selected AtLHL model via FlexX docking functionality (Gastreich et al. 2006; Trott and Olson 2010). A structural alignment was conducted by fragment assembly simulations based on iterative templates using the iterative threading assembly refinement (I-TASSER) server to match AtLHL to an experimentally confirmed structure in the PDB library (Zhang 2008). The model with the highest C-score was analysed using PyMOL (v.1.7.4.) (Schrödinger LLC, New York, USA) and then adopted in the study.

Cloning of the At3g18035 Gene

Total RNA was extracted from 6-week-old *A. thaliana* ecotype Columbia-0 (Col-0) seedlings using the RNeasy plant mini kit, in combination with DNase 1 treatment, as instructed by the manufacturer (Qiagen, Crawley, UK). At3g18035 cDNA synthesis from the total RNA and subsequent amplification of the AtLHL$^{301-480}$ gene fragment from the cDNA, were simultaneously performed in the presence of two sequence-specific primers (forward: 5′-GGAAGGCCT AGGAGAGTTGTTGACCCTAGC-3′ and reverse: 5′-GAA CAGAGCTTCTTGCATTGCCTCTGCTTC-3′), using a Verso 1-Step RT-PCR kit and in accordance with the manufacturer's instructions (Thermo Scientific, Rockford, USA). The PCR product was then cloned into a pTrcHis2-TOPO expression vector via the TA cloning system (Invitrogen Corp., Carlsbad, USA) to make a pTrcHis2-TOPO:AtLHL$^{301-480}$ fusion expression construct with a C-terminus His purification tag.

Expression of the AtLHL$^{301-480}$ Protein

For expression of the recombinant AtLHL$^{301-480}$ protein, competent *Escherichia coli* BL21 Star pLysS cells (Invitrogen, Carlsbad, USA) were transformed (through heat shock at 42 °C for 2 min) with the pCRT7/NT-TOPO:AtLHL$^{301-480}$ fusion construct and grown in double strength yeast-tryptone (2YT) media (16 g/L tryptone, 10 g/L yeast extract, 5 g/L NaCl and 4 g/L glucose; pH 7.0) containing 100 µg/ml ampicillin and 34 µg/ml chloramphenicol, on an orbital shaker (250 rpm) at 37 °C. Protein expression was induced by the addition of isopropyl-β-D-thiogalactopyranoside (IPTG, Sigma-Aldrich Corp., MO, USA) at a final concentration of 1 mM and when the optical density (OD_{600}) of the cell culture had reached 0.5 (approximately 3 h). The culture was then left to grow for a further 3 h at 37 °C.

Purification of the AtLHL$^{301-480}$ Protein

The resultant expressed recombinant AtLHL$^{301-480}$ protein was purified by preparing a cleared cell lysate of the induced *E. coli* cells under non-native denaturing conditions, whereby the harvested cells were resuspended in lysis buffer (8 M urea, 100 mM NaH_2PO_4, 10 mM Tris-Cl; pH 8.0, 500 mM NaCl, 20 mM β-mercaptoethanol, 7.5% (v/v) glycerol) at a ratio of 1 g pellet weight to every 10 ml buffer volume, mixed thoroughly using a mechanical stirrer at 24 °C for 1 h and then centrifuged at 2,500 × *g* for 15 min. Supernatant was collected as the cleared lysate and transferred to 2 ml of 50% (w/v) nickel-nitriloacetic acid (Ni-NTA) slurry (Sigma-Aldrich Corp., MO, USA) that had been pre-equilibrated with 10 ml of lysis buffer and the lysate/slurry mixture then gently swirled on a rotary mixer for 1 h at 24 °C. This step allowed for binding of the AtLHL$^{301-480}$ protein onto the Ni-NTA resin. The lysate–resin mixture was loaded into an empty XK16 column (Bio-Rad Laboratories Inc., CA, USA) and allowed to settle and flow-through discarded. The protein-bound resin was then washed three times with 30 ml of wash buffer (8 M urea, 100 mM NaH_2PO_4, 10 mM Tris-Cl; pH 8.0, 500 mM NaCl, 20 mM β-mercaptoethanol, 7.5% (v/v) glycerol and 40 mM imidazole) to remove unbound proteins.

Refolding of the AtLHL$^{301-480}$ Protein

The washed protein-bound resin was equilibrated with 2 ml of gradient buffer (8 M urea, 200 mM NaCl, 50 mM Tris-Cl; pH 8.0 and 20 mM β-mercaptoethanol) before the column was connected to a Bio-Logic F40 Duo-Flow chromatography system (Bio-Rad Laboratories Inc., CA, USA) programmed to run a linear refolding gradient. The refolding gradient for the denatured recombinant AtLHL$^{301-480}$ was then performed by linearly diluting the 8 M gradient buffer to 0 M urea concentration with a refolding buffer (200 mM NaCl, 50 mM Tris-Cl; pH 8.0, 500 mM glucose, 0.05% (w/v) polyethyl glycol, 4 mM reduced glutathione, 0.04 mM oxidized glutathione, 100 mM non-detergent sulfobetaine and 0.5 mM phenylmethanesulfonyl fluoride (PMSF)) over 10 h at a flow rate of 0.5 ml/min. After refolding, the renatured recombinant AtLHL$^{301-480}$ was eluted in 2 ml of elution buffer (200 mM NaCl, 50 mM Tris-Cl; pH 8.0, 250 mM imidazole, 20% (v/v) glycerol and 0.5 mM PMSF). The eluted native protein fraction was then de-salted and concentrated using a Spin-XUF filtration/concentration device with a molecular weight cut-off (MWCO) point of 3000 Da and in accordance with the manufacturer's instructions (Corning Corp., NY, USA).

Protein concentration was determined by the Bradford method (Bradford 1976) and ND2000 nanodrop spectrophotometer (Thermo Scientific Inc., MA, USA) before the recombinant protein was stored at −20 °C.

Testing for the In Vitro AC Activity of AtLHL$^{301-480}$

The probable in vitro AC activity of the purified recombinant AtLHL$^{301-480}$ was tested by incubating 5 µg of the protein in 50 mM Tris-Cl (pH 8.0) containing 5 mM Mg^{2+} or Mn^{2+} and 1 mM ATP, with or without 250 µM Ca^{2+} or 50 mM HCO_3-, in a final volume of 200 µl, followed by measurement of the generated cAMP. Background cAMP levels in control reactions were measured in tubes containing all the other components but no protein or Ca^{2+} or HCO_3-. All incubations were performed at room temperature (24 °C) for 20 min and terminated by the addition of 10 mM EDTA followed by boiling for 3 min and cooling on ice for 2 min before centrifugation at 2,500 × *g* for 3 min. The resulting supernatants were assayed for cAMP content using the cAMP-linked enzyme linked immunosorbent assay (ELISA) kit, following its acetylation protocol and as is described by the supplier's manual (Sigma-Aldrich Corp., MO, USA; code: CA201). The anti-cAMP antibody in this assaying system is highly specific for cAMP and has approximately a 10^6 times lower affinity for 3′,5′-cyclic guanosine monophosphate (cGMP). In all cases, each experiment was performed in triplicate ($n = 3$) using three different protein extracts that had been independently prepared.

Detection of cAMP by Mass Spectrometry

Acetylated cAMP samples from the in vitro AC activity assays were also assayed by tandem liquid chromatography mass spectrometry (LC-MS/MS). In this method, samples were introduced into a Waters API Q-TOF Ultima mass spectrometer (Waters Microsep, Johannesburg, RSA) with a Waters Acquity UPLC at a flow rate of 180 ml/min. Separation was achieved in a Phenomenex Synergi (Torrance, CA) 4 µm Fusion-RP (250 × 2.0 mm) column when a gradient of solvent 'A' (0.1% formic acid) and solvent 'B' (100% acetonitrile) was applied over 18 min. During the first 7 min, the solvent composition was kept at 100% 'A' followed by a linear gradient of up to 80% 'B' for 3 min and then a re-equilibration to the initial conditions. An electrospray ionization in the negative (W-) mode was used at a cone voltage of 35 V, to detect molecules and generate chromatograms.

Testing for the Ability of AtLHL$^{301-480}$ to Complement *cya*A Mutation in *E. coli*

The *E. coli* mutant strain, SP850 (lam-, el4-, relA1, spoT1, *cya*A1400 (:kan), thi-1) (Shah and Peterkofsky 1991; Ullmann and Danchin 1983), deficient in the AC gene (*cya*A), was obtained from the *E. coli* Genetic Stock Centre (Yale University, New Haven, USA; accession No. 7200). The strain was prepared to be chemically competent followed by its transformation with the pTrcHis2-TOPO:AtLHL$^{301-480}$ fusion construct (through heat shock at 42 °C for 2 min). The transformed bacteria together with the non-transformed cells were then grown at 37 °C in Luria-Bertani (LB) media containing kanamycin (15 µg/ml) up until their cell culture had reached an optical density (OD_{600}) of 0.5. Both groups of cells were streaked on MacConkey agar supplemented with 15 µg/ml kanamycin and 0.5 mM IPTG (Sigma-Aldrich Corp., Missouri, USA) (for transgene induction) before the streaked media was incubated for 40 h at 37 °C, for visual evaluation. After incubation, an ability of the induced transformed mutant cells to now ferment lactose would then be considered as an indication of the expressed recombinant AtLHL$^{301-480}$'s ability to generate cAMP from ATP, as a functional AC. As a result, the induced transformed cells would turn deep red or purple (just like wild-type cells), while the mutant control cells would remain yellowish or colourless (Shah and Peterkofsky 1991; Ullmann and Danchin 1983).

Electrochemical Evaluation of the In Vitro AC Activity of AtLHL$^{301-480}$

Various electrodes were prepared in a 20 ml cell system, using GCE bio-electrodes (BioAnalytical Systems, West Lafayette, IN, USA) (polished with 1.0, 0.3 and 0.05 µm alumina (Buehler, IL, USA)) and washed with distilled water before ultrasonication for 5 min in distilled water and 5 min in ethanol, and drying in a stream of N_2 for 10 s before drop coating), whereby the control electrode (a 0.071 cm^2 glassy carbon (GCE)) was left uncoated, whereas the basal electrode (a Ag/AgCl platform with a 3 M NaCl salt bridge (GCE)) was coated with the AtLHL$^{301-480}$ protein (5 µg) while test electrodes (auxiliary platinum wires (GCE)) were each coated with the AtLHL$^{301-480}$ protein (5 µg) pre-incubated with each of the selected and tested AC co-factors (5 mM Mg^{2+} or Mn^{2+}) or modulators (250 µM Ca^{2+} or 50 mM HCO_3-). These electrodes were then connected to a BAS Epsilon electrochemical workstation (BioAnalytical Systems, West Lafayette, IN, USA), followed by recording of the resultant square wave voltammetries with a computer interface linked to the workstation at a potential scan rate of 2 mVs^{-1} from the initial potential to the $E_i = +300$ mV switch potential, and the $E_\lambda = 350–1000$ mV experimental potential. Wherever there was binding of a co-factor or modulator by the protein, the reading of such a test coated electrode would be expected to be higher than that of the uncoated control electrode and that of the basal electrode coated with the AtLHL$^{301-480}$ alone. All experiment

recordings were carried out at 25 °C at a constant amplitude of 25 mV and a fixed frequency of 15 mV. The method is further detailed elsewhere (Mulaudzi et al. 2011).

Searching for Calcium-Binding Sites in AtLHL

Three different methods were used for this task. In the first method, AtLHL sequence was manually searched for presence and frequency of the 9-residue calcium-binding site commonly known as the RTX (repeat-in-toxin) motif, GGXGXDXHX, where X is any amino acid and H is any hydrophobic residue (Grzybowska 2018). In the second method, AtLHL sequence was aligned with five selected Arabidopsis proteins (At1g05990, At3g43810, At2g17290, At5g23580 and At4g23650) containing the EF-hand motif (Grzybowska 2018) to which calcium binds, followed by homology search using MAFFT (https://mafft.cbrc.jp/alignment/server/) (Katoh et al. 2019). In the last method, the prediction program of the Calmodulin Target Database (http://calcium.uhnres.utoronto.ca/) was used to search for presence and frequency of the 17-residue calmodulin-binding site; KLWKKLLKLLKKLLKLG (Kauer et al. 1986) in the AtLHL sequence. The program predicts the calmodulin-binding site sequences based on criteria such as hydropathy, α-helical propensity, residue weight, residue charge, hydrophobic residue content and helical and occurrence of particular residues. In this regard, sequences are scored from 0 to 9, with the most likely binding site assigned a series of 9 s (Yap et al. 2000).

Searching for the AC Centre in Other LH Family Proteins

Amino acid sequences of AtH2A, AtH2B, AtH3 and AtH4 were retrieved from TAIR (https://www.arabidopsis.org/). The retrieved sequences were uploaded to the MAFFT online alignment tool (https://mafft.cbrc.jp/alignment/server/) and then alignment ran with default settings to search for sequence similarities at the AC centre.

Reaction Kinetics of the Recombinant AtLHL$^{301-480}$ Protein

Individual reaction settings of the increasing concentration of ATP (0.0; 0.5; 1.0; 1.5 and 2.0 mM) were prepared in 200 µl of 50 mM Tris-Cl (pH 8.0) containing 5 µg AtLHL and 5 mM Mn^{2+}, followed by incubation at room temperature (24 °C) for 20 min. After incubation, each reaction was terminated by the addition of 10 mM EDTA followed by boiling for 3 min and cooling on ice for 2 min before centrifugation at 2500 × *g* for 3 min. The resulting supernatants were then assayed for cAMP content using the cAMP-linked ELISA kit, following its acetylation protocol as is instructed by the supplier (Sigma-Aldrich Corp., MO, USA; code: CA201). The initial velocity for each of the used ATP concentrations was then used to sketch a Hanes plot, followed by determination of the reaction kinetic constants (K_m and V_{max}) of AtLHL$^{301-480}$ from the same plot. K_m was determined as the negative value of the *x*-intercept ($x = -K_m$, when $y = 0$) of a linear fit of the data, while V_{max} was calculated from the *y*-intercept ($y = K_m/V_{max}$, when $x = 0$) of the same linear fit (Irving et al. 2012).

Statistical Analysis

All generated enzyme immunoassaying data was subjected in triplicate sets ($n = 3$) to one-way analysis of variance (ANOVA) (Super-Anova, Statsgraphics version 7, 1993; Statsgraphics Corp., The Plains, VI, USA). Wherever ANOVA revealed significant differences between treatments, means were separated by *post hoc* Student–Newman–Keuls (SNK) multiple range test ($p < 0.05$).

Results

Structure and Computational Analysis of AtLHL and its AC Centre

The identification of ACs in plants has mostly involved querying protein sequences with an AC motif (Fig. 1A) derived from a guanylyl cyclase (GC) search motif (Ludidi and Gehring 2003) through modification at position 3, changing [CTGH] to [DE] (Gehring 2010). This modification is primarily based on previous findings, which indicate that the conversion of GCs into ACs and vice versa could be easily achieved through a single mutation in the amino acid that confers substrate specificity (Tucker et al. 1998; Roelofs et al. 2001). In this study, when the amino acid sequence of AtLHL was queried by the AC motif, a matching hit was detected towards its C-terminal end (amino acids 382–399) (Fig. 1B). We also submitted the whole AtLHL sequence to ACPred, which is available at http://gcpred.com/acpred/ (Xu et al. 2018), for prediction of the AC centre in the AtLHL protein. The software then identified the region K382 to D399 (Fig. 1B) that fits the [RKS]X[DE]X{9,11}[KR]X{1,3}[DE] AC motif (Fig. 1A) and its search hit (Fig. 1B). Next, computational analysis of the AtLHL protein was undertaken to assess and determine the ability of its AC centre to bind ATP and catalyse its subsequent conversion into cAMP. The full-length model of AtLHL was prepared by artificial intelligence followed by docking simulations, which then showed that in this model, the AC centre is solvent-exposed, thus allowing for unimpeded substrate interactions and ultimately catalysis (Zhou et al. 2021) (Fig. 1C–F).

(A) **Search motif:**

```
--[RKS]X[DE]X{9,11}[KR]X{1,3}[DE]--
    1  2  3        12/14
```

(B) **Amino acid sequence**

```
1                                                                    70
MDPSLGDPHHPPQFTPFPHFPTSNHHPLGPNPYNNHVVFQPQPQTQTQIPQPQMFQLSPHVSMPHPPYSE
MICAAIAALNEPDGSSKMAISRYIERCYTGLTSAHAALLTHHLKTLKTSGVLSMVKKSYKIAGSSTPPAS
VAVAAAAAAQGLDVPRSEILHSSNNDPMASGSASQPLKRGRGRPPKPKPESQPQPLQQLPPTNQVQANGQ
PIWEQQQVQSPVPVPTPVTESAKRGPGRPRKNGSAAPATAPIVQASVMAGIMKRRGRPPGRRAAGRQRKP
KSVSSTASVYPYVANGARRRGRPRRVVDPSSIVSVAPVGGENVAAVAPGMKRGRGRPPKIGGVISRLIMK
PKRGRGRPVGRPRKIGTSVTTGTQDSGELKKKFDIFQEKVKEIVKVLKDGVTSENQAVVQAIKDLEALTV
TETVEPQVMEEVQPEETAAPQTEAQQTEAAETQGGQEEGQEREGETQTQTEAEAMQEALF
```

(C)

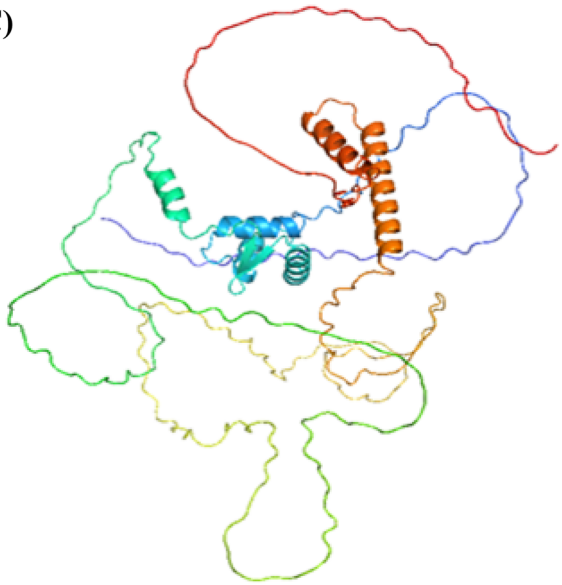

(D)

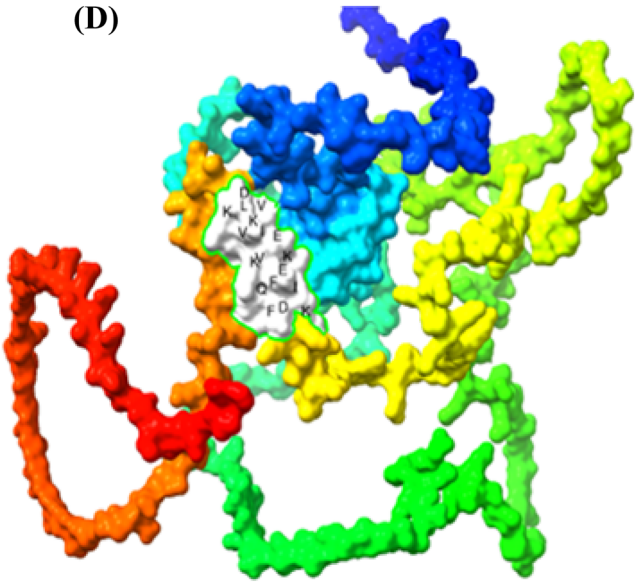

(E)

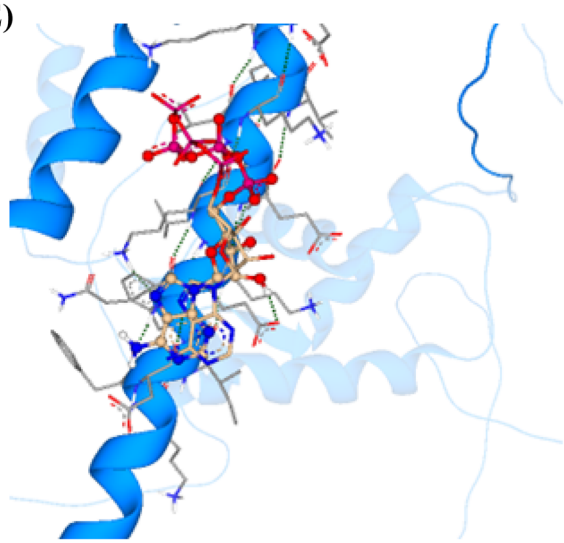

(F)

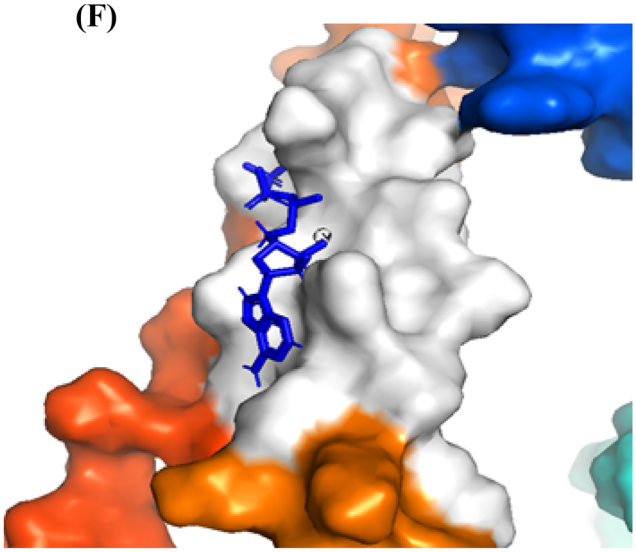

◂**Fig. 1** Structural features and computational analysis of AtLHL. **A** The 14 amino acid AC search motifs derived from annotated and experimentally tested GC and AC catalytic centres (Ludidi and Gehring 2003; Gehring 2010). The residue forming hydrogen bonding with purine at position 1 is highlighted in red; the residue conferring substrate specificity in position 3 is highlighted in blue; while the amino acid in position 14, stabilizing the transition state from ATP to cAMP, is highlighted in red. The amino acid [DE] at 1–3 residue downstream from position 14 participates in Mg^{2+}/Mn^{2+}-binding and is coloured green (Ludidi and Gehring 2003; Gehring 2010). **B** The complete amino acid sequence of AtLHL with the AC catalytic centre towards its C-terminus (amino acids 382–399) highlighted in bold and underline, and the 180 amino acid sequence fragment expressed and tested for AC activity indicated within the inverted red triangles. **C** 3D rainbow depiction of the AtLHL ribbon model as affirmed by PyMOL, where the N→C orientation is shown as blue→red. **D** Surface model (crystal structure) of AtLHL, highlighting the solvent-exposed AC centre (white), wherein residues of the centre are labelled with single letter codes in black. Docking of ATP at the AC centre and interaction of ATP with key residues in the catalytic centre of AtLHL shown as stick (tail) and dots (head) in the ribbon model **E**, and club (phosphate) and ball (purine) in the surface model **F**. AtLHL was modelled using AlphaFOLD (Varadi et al. 2022), while ATP docking simulation was performed using the FlexX functionality of SeeSAR (v12.0.1) (Gastreich et al. 2006)

Testing and Confirmation of the AC Activity of AtLHL$^{301-480}$

To assess the AC activity of AtLHL, a fragment sequence of the At3g18035 gene (amino acids 301–480), harbouring the AC motif (Fig. 1B), was cloned into a prokaryotic system and expressed into a 23.300 kDa AtLHL$^{301-480}$ His-tagged recombinant protein (Fig. 2A). To check if the AC centre of AtLHL can generate cAMP in vitro, the expressed recombinant AtLHL$^{301-480}$ was affinity purified (Fig. 2B, left inset) and tested in a reaction mixture containing ATP as substrate, Mn^{2+} or Mg^{2+} as co-factor and Ca^{2+} or HCO_3- as modulator, followed by measurement of cAMP by enzyme immunoassay. Maximum activity was reached after 20 min of the reaction system (Fig. 2B, right inset), generating about 103.25 fmols/µg protein of cAMP in the presence of Mn^{2+} and approximately 21.50 fmols/µg protein of cAMP in the presence of Mg^{2+} compared to only about 15.15 fmols/µg protein of cAMP of the control reaction (Fig. 2B). Besides being strictly Mn^{2+}-dependent, the catalytic activity of AtLHL$^{301-480}$ was also significantly enhanced by both Ca^{2+} and HCO_3-, reaching activity levels of around 150.00 and 126.50 fmols/µg protein of cAMP respectively when Mn^{2+} is the co-factor (Fig. 2B). cAMP was also measured by LC-MS/MS, and in a reaction mixture containing AtLHL$^{301-480}$, ATP and Mn^{2+}, the product was detected (Fig. 2C) at almost 90% level of cAMP (Fig. 2D). This additional method, therefore, confirmed presence of cAMP in the reaction mixture, thus validating the ELISA technique and, at the same time, confirming AC activity for the recombinant AtLHL$^{301-480}$ protein.

To check if the AC centre of AtLHL can rescue AC-deficiency in *E. coli*, the AtLHL$^{301-480}$ protein was expressed in the *E. coli* host strain, SP850, lacking the AC gene (*cya*A), essential for lactose fermentation (Shah and Peterkofsky 1991; Ullmann and Danchin 1983). As a result of this mutation, the SP850 mutant cells remained yellowish in colour when grown on MacConkey agar, while in contrast, the AtLHL$^{301-480}$-expressing SP850 cells formed deep reddish colonies (Fig. 2E) much like what wild-type *E. coli* does (Shah and Peterkofsky 1991; Ullmann and Danchin 1983). This thus, indicated a functional AC centre in AtLHL.

Characterization of the AC Activity of AtLHL$^{301-480}$

To check if AtLHL physically interacts with its catalytic co-factors or modulators during catalysis and/or activation, AtLHL$^{301-480}$ alone or AtLHL$^{301-480}$ pre-incubated with individual co-factors or modulators was used to coat electrodes, followed by recording of square wave voltammetries using a computer interface linked to a workstation at a potential scan rate of 2 mVs^{-1} from the initial potential to the $E_i = +300$ mV switch potential and the $E_\lambda = 350–1000$ mV experimental potential. Peak detection occurred at around 0.23 V, whereby the control bare electrode showed a peak of ~1.27 A, while AtLHL$^{301-480}$ alone, AtLHL$^{301-480}$ plus Mg^{2+}, AtLHL$^{301-480}$ plus Mn^{2+}, AtLHL$^{301-480}$ plus HCO_3- and AtLHL$^{301-480}$ plus Ca^{2+} showed peaks of ~1.73, ~1.99, ~2.25, ~3.26 and ~5.00 A, respectively (Fig. 3A), thus signifying physical interaction between AtLHL and its catalytic co-factors or modulators. Since the co-factor binding site of AtLHL was already known to exist within its AC centre (Gehring 2010), we then sought to search for the possible existence of the calcium binding site or sites within this protein so that this could better explain the observed physical interaction between AtLHL$^{301-480}$ and its catalytic modulators. Using the Calmodulin Target Database program (http://calcium.uhnres.utoronto.ca/) that predicts calmodulin-binding site sequences (Yap et al. 2000) based on various criteria (Kauer et al. 1986) to search the AtLHL amino acid sequence, a single 16-residue calmodulin-binding sequence (IVQASVMAGIMKRRGR) was identified as the most likely binding site for Ca^{2+} in AtHLH (Fig. 3B). Finally, the reaction kinetics of AtLHL as functional AC enzyme were then calculated, and a K_m constant of around 0.7 mM and V_{max} constant of approximately 9.2 fmol/min/µg protein were obtained (Fig. 3C).

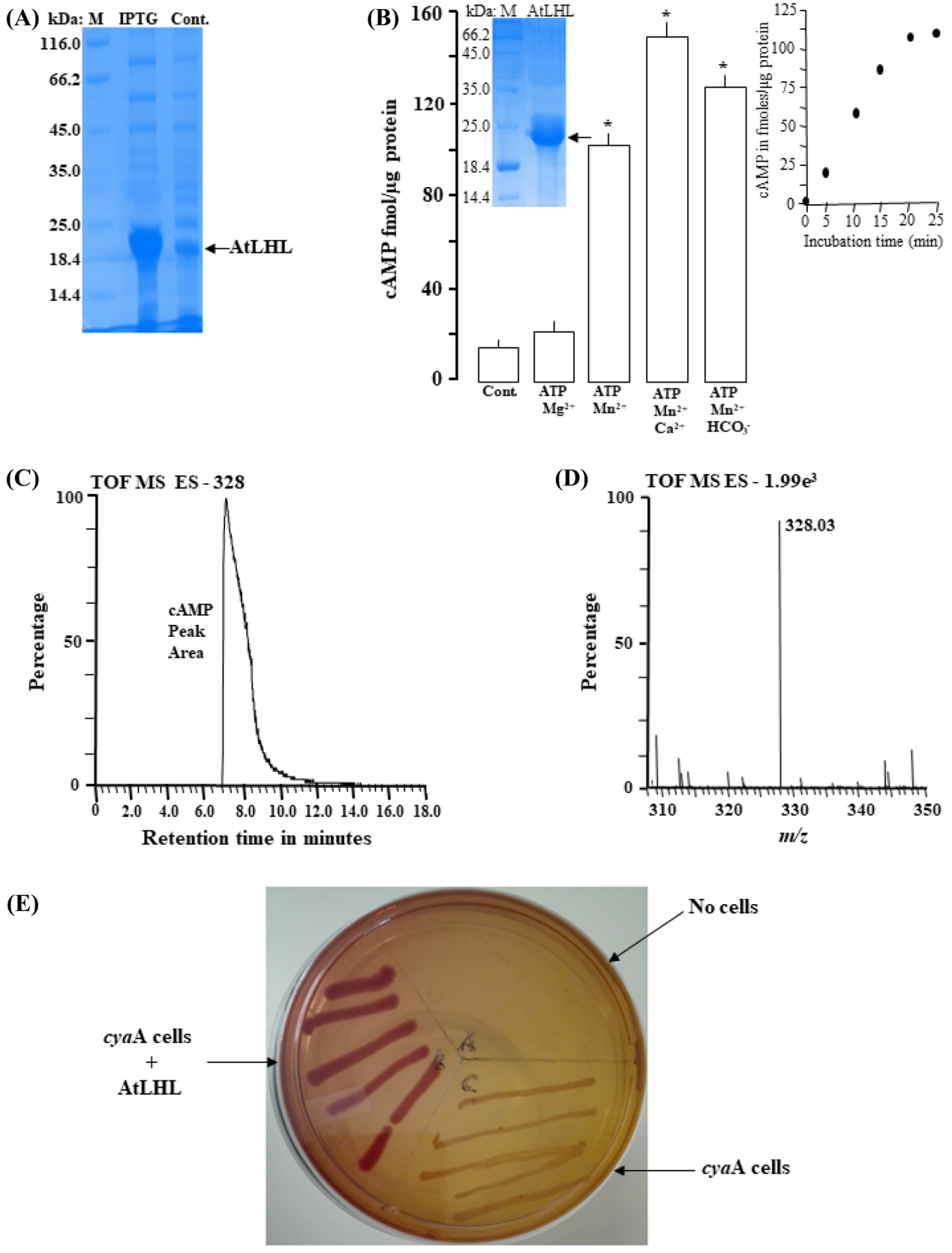
(A)
kDa: M IPTG Cont.
116.0
66.2
45.0
35.0
25.0
18.4
14.4
AtLHL
(B)
kDa: M AtLHL
66.2
45.0
35.0
25.0
18.4
14.4
cAMP fmol/µg protein
160
120
80
40
0
Cont.
ATP Mg2+
ATP Mn2+
ATP Mn2+ Ca2+
ATP Mn2+ HCO3-
cAMP in fmoles/µg protein
125
100
75
50
25
0
0 5 10 15 20 25
Incubation time (min)
(C)
TOF MS ES - 328
100
50
0
Percentage
cAMP Peak Area
0 2.0 4.0 6.0 8.0 10.0 12.0 14.0 16.0 18.0
Retention time in minutes
(D)
TOF MS ES - 1.99e3
328.03
100
50
0
Percentage
310 320 330 340 350
m/z
(E)
No cells
cyaA cells + AtLHL
cyaA cells

◂**Fig. 2** Testing and confirmation of the AC activity of AtLHL$^{301-480}$. **A** Sodium dodecyl sulphate–polyacrylamide gel electrophoresis (SDS-PAGE) of protein fractions (stained with Coomassie brilliant blue) from the induced (IPTG) and un-induced (Cont.) cell cultures, where (M) is the molecular weight marker and the arrow marking the expressed recombinant AtLHL$^{301-480}$ protein. **B** cAMP generated by 5-µg recombinant AtLHL$^{301-480}$ in the presence of 1 mM ATP and 5 mM Mg^{2+} or Mn^{2+} or 1 mM ATP and 250 µM Ca^{2+} or 50 mM HCO_3- when 5 mM Mn^{2+} ion is the co-factor. Control reaction contained all other components except the protein, Ca^{2+}, and HCO_3-. Left insert: a Coomassie brilliant blue-stained gel after resolution of the affinity purified His-tagged recombinant AtLHL$^{301-480}$ (arrow) by SDS-PAGE. Right insert: time course calibration curve. Data are mean values ($n=3$) and error bars show standard error (SE) of the mean. Asterisks denote values significantly different from those of control ($p<0.05$) determined by the analysis of variance (ANOVA) and *post hoc* Student–Newman–Keuls (SNK) multiple range tests. **C** An extracted mass chromatogram of the *m/z* 328 $[M-1]^{-1}$ ion of cAMP generated by 5 µg of AtLHL$^{301-480}$ in a reaction system containing 50 mM Tris-Cl; pH 8.0, 1 mM ATP, and 5 mM Mn^{2+} after 20 min. **D** Mass of the resultant cAMP peak in the chromatogram. **E** The AC centre of AtLHL$^{301-480}$ complemented the *cya*A mutant *E. coli* (SP850) to ferment lactose. AtLHL$^{301-480}$-expressing SP850 *E. coli* cells showed a strong reddish colour as if they were wild-type cells (Shah and Peterkofsky 1991; Ullmann and Danchin 1983), while *cya*A mutant cells yielded yellowish colonies

Discussion

Adenylyl cyclases (ACs) are enzymes capable of catalysing the conversion of adenosine 5′-triphosphate (ATP) to the second messenger, 3',5'-cyclic adenosine monophosphate (cAMP) (Robison et al. 1968; Goodman et al. 1970; Gerisch et al. 1975). In plants, cAMP in turn controls various downstream processes such as the cell cycle (Ehsan et al. 1998), growth of pollen tubes (Tezuka et al. 1993; Malho et al. 2000; Moutinho et al. 2001; Vaz Dias et al. 2019) and response to stress (Jin and Wu 1999; Ma et al. 2009; Sabetta et al. 2019; Blanco et al. 2020). Across the different species of land plants on earth (ranging from mosses and herbs to woods), a total of twenty-nine ACs have so far been identified, using various methods (Yuan et al. 2022; Liu et al. 2023). Apparently, while methods such as omics analysis and homologous cloning have been successfully used to identify ACs in other plants, the discovery of ACs in *Arabidopsis thaliana*, *Glycine max* and *Physcomitrella patens* has mostly been through a systematic approach, which involved identification of key amino acid residues in the catalytic centre of known and experimentally tested nucleotide cyclases (NCs) (Ludidi and Gehring 2003). In that approach, a GC search motif (Ludidi and Gehring 2003) at position 3 was changed from [CTGH] to [DE] to generate a rationally designed search motif specific for ACs (Fig. 1A) (Gehring 2010). This substitution was based on previous findings, which indicated that the conversion of GCs into ACs and vice versa could be achieved by a single mutation in the amino acid residue that confers substrate specificity (Tucker et al. 1998; Roelofs et al. 2001).

Using this systematic approach, a total of sixteen ACs have been discovered, i.e. eleven in *A. thaliana*, four in *P. patens* and only one in *G. max*. The Arabidopsis ACs are AtPPR-AC (Ruzvidzo et al. 2013), AtKUP7 (Al-Younis et al. 2015), AtClAP (Chatukuta et al. 2018), AtKUP5 (Al-Younis et al. 2018), AtLRRAC1 (Bianchet et al. 2019; Ruzvidzo et al. 2019), AtNCED3 (Al-Younis et al. 2021), AtAC (Sehlabane et al. 2022), AtMEE (Kawadza et al. 2022) and AtTIR1, AtAFB1 and AtAFB5 (Qi et al. 2022), while the moss ACs are PpAFB1, PpAFB2, PpAFB3 and PpAFB4 (Qi et al. 2022), and the soybean AC is GmAC (Bobo et al. 2022). AtPPR-AC is annotated to play a role in chloroplast biogenesis and the restoration of cytoplasmic male sterility (CMS) (Ruzvidzo et al. 2013), while AtClAP is predicted to have a role in endocytosis and plant defence (Chatukuta et al. 2018). The two AtKUPs are responsible for K^+ ion flux (Al-Younis et al. 2015, 2018). AtLRRAC1 has a role in pathogen defence (Bianchet et al. 2019; Ruzvidzo et al. 2019), while AtNCED3 is involved in the biosynthesis of the stress hormone abscisic acid (ABA) (Al-Younis et al. 2021). AtAC is known to be transcriptionally upregulated in response to biotic stress (Sehlabane et al. 2022), while AtMEE is involved in embryogenesis and response to abiotic stress (Kawadza et al. 2022). TIR1 and all the AFB ACs from *A. thaliana* and *P. patens* are auxin receptors involved in the regulation of root growth mediated by auxin (Qi et al. 2022), while GmAC has a role in early plant development and stress response (Bobo et al. 2022).

Apparently, there are also four other plant ACs, discovered through either the omics analysis or homologous cloning methods, that harbour the same rationally designed AC search motif, i.e. two from *Zea mays*, one from *Nicotiana benthamiana* and one from *A. thaliana*. The maize ACs are ZmPSiP (Moutinho et al. 2001) and ZmRPP13-LK3 (Yang et al. 2021), while the tobacco AC is NbAC (Ito et al. 2014), and the Arabidopsis AC is AtDK4 (Vaz Dias et al. 2019). ZmPSiP is responsible for the polarized growth and re-orientation of pollen tubes (Moutinho et al. 2001), while ZmRPP13-LK3 participates in ABA-mediated resistance to heat stress (Yang et al. 2021). NbAC has a role in tabtoxinine-β-lactam-induced cell death during the development of wildfire disease (Ito et al. 2014) while AtDK4 plays a role in nitric oxide (NO)-dependent pollen tube guidance and fertilization (Vaz Dias et al. 2019).

Notably, besides these twenty ACs harbouring the rationally designed AC search motif across all plants, nine other plant ACs, all lacking the rationally designed AC search motif, are known. These include one from *Hippeastrum hybridum*, which is HpAC1 (Świeżawska et al. 2014); one from *Marchantia polymorpha* that is MpAC (Kasahara et al. 2016); two from *Brachypodium distachyon*, namely, BdTTM3 and BdGUCD1 (Świeżawska et al. 2020; Duszyn et al. 2022); two from *Malus domestica*, namely, MdTTM1 and MdTTM2

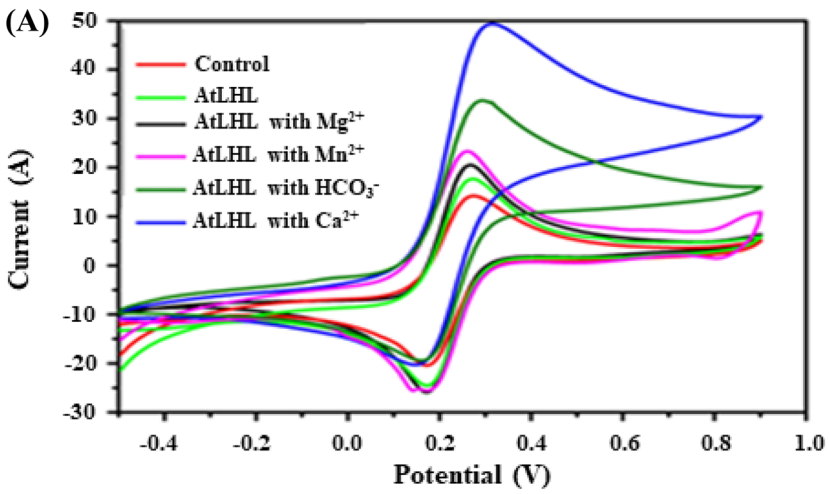

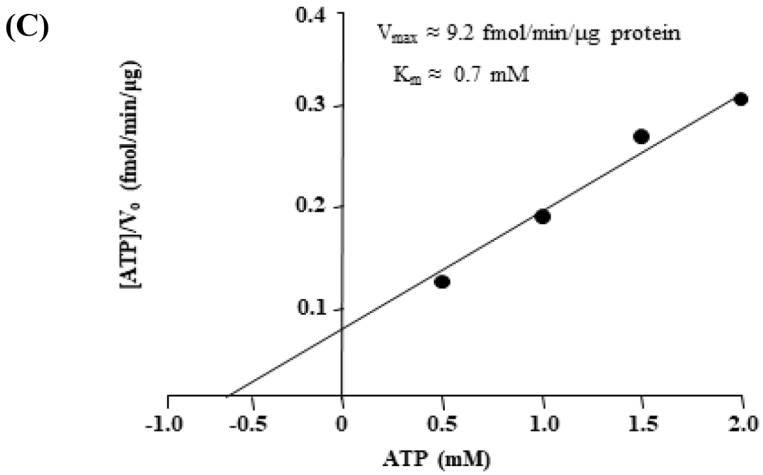

Fig. 3 Characterization of the AC activity of AtLHL$^{301-480}$. **A** Square wave voltammograms showing the response of AtLHL$^{301-480}$ in 5 ml of 50 mM Tris-HCl buffer (pH 8.0) when it is on its own (lime green) or after its pre-incubation with either 5 mM Mg^{2+} (black) or 5 mM Mn^{2+} (pink) or 50 mM HCO_3- (green) or 250 µM Ca^{2+} (blue). The square wave voltammogram of the uncoated/bare control electrode is shown in red. The used potential window was −0.35 to 1.0 V, while the scan rate was 2 mVs^{-1}. The scan shows peaks at ~0.23 V. **B** Prediction of Ca^{2+} binding sites in AtLHL using the Calmodulin Target Database program, showing a single 16-residue calmodulin-binding sequence (IVQASVMAGIMKRRGR) as the only most likely binding site (blue). **C** Hanes plot for the determination of the reaction kinetics of AtLHL, whereby *K*m was determined as the negative value of the *x*-intercept ($x=-K_m$, when $y=0$) of the linear fit and V_{max} calculated from the *y*-intercept ($y=K_m/V_{max}$, when $x=0$) of the same linear fit

(Yuan et al. 2022); and three from *Ziziphus jujuba*, which are ZjAC1, ZjAC2 and ZjAC3 (Liu et al. 2023). HpAC1 is involved in responses to infection by the plant fungal pathogen, *Phoma narcissi*, and also injuries through mechanical damage (Świeżawska et al. 2014), while MpAC has a role in male organ and cell development (Kasahara et al. 2016). BdTTM3 is responsible for responses to mechanical wounding (Świeżawska et al. 2020), while BdGUCD1 is involved in jasmonic acid (JA)-mediated responses to *Fusarium pseudograminearum* infection (Duszyn et al. 2022). MdTTM1 and MdTTM2 currently do not have any known function(s) (Yuan et al. 2022), while ZjAC1, ZjAC2 and ZjAC3 are involved in the significant acceleration of seed germination, root growth and flowering, respectively (Liu et al. 2023).

Interestingly, in *A. thaliana*, there exists another additional protein annotated to be an AC at NCBI (https://www.ncbi.nlm.nih.gov/protein/51968402). This protein, termed linker histone-like (AtLHL) or HON4 protein, coded for by the At3g18035 gene, has the rationally designed AC search motif (Fig. 1B), however, has never been functionally confirmed as an AC. This is also despite the fact that the protein is known to be primarily involved in a number of key cellular processes essentially mediated by cAMP. Such processes include (i) chromatin formation, where AtLHL binds to the nucleosome and linker DNA (Jeon and Berezney 1995); (ii) embryogenesis, where the protein controls the expression of pluripotency genes (Martianov et al. 2005); (iii) reproduction, where AtLHL controls the differentiation of sperm cells (Tanaka et al. 2003); and (iv) disease resistance, where the protein regulates the innate immune and stress response genes (Studencka et al. 2011) and drought stress response (Ascenzi and Gantt 1997; Scippa et al. 2000; Wu et al. 2022). Therefore, based on this basis, we then sought to assess and establish if this additional Arabidopsis protein candidate could also be a functional AC.

We then started the assessment by using ACPred, which is a prediction tool designed to identify motif-based AC centres in proteins with multiple domains (Xu et al. 2018), to predict the presence and location of the AC centre in AtLHL. Supported with the 3D model of AtLHL generated by AlphaFOLD using artificial intelligence (Varadi et al. 2022), the identified centre was found to encompass amino acid residues K382 to D399 (Fig. 1C and D), which furthermore, concurred with the information and data from NCBI (https://www.ncbi.nlm.nih.gov/protein/51968402). The FlexX functionality of SeeSAR (v12.0.1) (Gastreich et al. 2006) was then used to carry out docking simulations of the substrate ATP at this AC centre, and the software predicted good affinity for the ATP at the centre (Fig. 1E and F). Additionally, both the artificial intelligence and SeeSAR showed that in the AtLHL model, the AC centre is solvent-exposed, thus indicating its unimpeded access to the centre and ultimately catalysis (Zhou et al. 2021). Notably, this same outcome is so much consistent with what was also obtained previously for AtKUP7 (Al-Younis et al. 2015), AtClAP (Chatukuta et al. 2018), AtKUP5 (Al-Younis et al. 2018), AtLRRAC1 (Bianchet et al. 2019; Ruzvidzo et al. 2019), AtNCED3 (Al-Younis et al. 2021), AtAC (Sehlabane et al. 2022) and MdTTM1 and MdTTM2 (Yuan et al. 2022).

We then cloned a fragment of the At3g18035 gene and expressed a truncated version of the AtLHL protein ($AtLHL^{301-480}$) harbouring the AC search motif (Fig. 1B) as a His-tagged fusion recombinant product of approximately 23.300 kDa (Fig. 2A). When purified (Fig. 2B, left inset) and tested for in vitro AC activity, using ELISA, after a 20-min reaction time (Fig. 2B, right inset), the recombinant $AtLHL^{301-480}$ showed a Mn^{2+}-dependent activity that is positively enhanced by Ca^{2+} and HCO_3- ions (Fig. 2B). This very same result was also obtained via LC-MS/MS (Fig. 2C and D), another analytical method capable of specifically and sensitively detecting cAMP levels at femtomolar concentrations, thus validating the ELISA technique and also confirming the AC activity of the $AtLHL^{301-480}$ recombinant protein.

In order to validate the AC activity of AtLHL (detected by ELISA and confirmed by LM-MS/MS), recombinant $AtLHL^{301-480}$ was expressed in a *cya*A *Escherichia coli* mutant strain (SP850) to see if it could rescue the mutant. This mutant strain has a catabolic defect of lacking the only AC system available in *E. coli*, necessary for lactose fermentation; therefore, its rescue by any foreign protein to metabolize lactose signifies AC function for such a protein (Shah and Peterkofsky 1991; Ullmann and Danchin 1983). In our case, $AtLHL^{301-480}$ rescued the SP850 strain (Fig. 2E), thereby validating the AC function of AtLHL. Notably, this outcome is also very much consistent with what was previously obtained for ZmPSiP (Moutinho et al. 2001), AtPPR-AC (Ruzvidzo et al. 2013), HpAC1 (Świeżawska et al. 2014), AtKUP7 (Al-Younis et al. 2015), MpAC (Kasahara et al. 2016), AtClAP (Chatukuta et al. 2018), AtKUP5 (Al-Younis et al. 2018), AtLRRAC1 (Bianchet et al. 2019; Ruzvidzo et al. 2019), ZmRPP13-LK3 (Yang et al. 2021), BdTTM3 (Świeżawska et al. 2020), AtNCED3 (Al-Younis et al. 2021), AtAC (Sehlabane et al. 2022), MdTTM1 and MdTTM2 (Yuan et al. 2022), AtAFB1 and AtAFB5 (Qi et al. 2022), GmAC (Bobo et al. 2022), AtMEE (Kawadza et al. 2022) and ZjAC1, ZjAC2 and ZjAC3 (Liu et al. 2023).

Apparently, the observed outcome whereby $AtLHL^{301-480}$ exhibited a relatively higher (~4.6-fold) in vitro AC activity with Mn^{2+} as opposed to Mg^{2+} (Fig. 2B), proposes that AtLHL could be a soluble AC (sAC) because all sACs prefer Mn^{2+} to Mg^{2+} ion as a co-factor of activity and are intracellularly localized (Braun and Dods 1975; Steer and Levitzki 1975; Sehlabane et al. 2022). In *A. thaliana*, AtLHL is localized in the nucleus (https://www.arabidopsis.org/) just like all other known sACs (Sehlabane et al. 2022). Moreover, the subsequent activation of $AtLHL^{301-480}$ by both calcium (~1.5-fold) and hydrogen carbonate (~1.2-fold)

(Fig. 2B), further points to our earlier assumption that AtLHL could be a sAC because only sACs and not transmembrane ACs (tmACs) are functionally activated by the Ca^{2+} and HCO_3- ions (Chen et al. 2000; Kamenetsky et al. 2006; Sehlabane et al. 2022); whereby activation by Ca^{2+} is through physical interaction via a Ca^{2+}-binding protein (calmodulin) (Kamenetsky et al. 2006), whereas that by HCO_3- is thought to be through the alteration of pH (Chen et al. 2000). Interestingly, the molecular interaction of $AtLHL^{301-480}$ with either its co-factors (Mg^{2+} and Mn^{2+}) or modulators (Ca^{2+} and HCO_3-) during its catalysis or activation, respectively, was actually found to be physical (Mulaudzi et al. 2011) (Fig. 3A), proposing for the possible presence of Mg^{2+}, Mn^{2+}, Ca^{2+} and/or HCO_3- binding sites in this protein.

Arguably, the probable existence of Ca^{2+} binding sites in AtLHL and its associated activation by this very same metal ion, strongly prompted our interest to search for such sites in the protein. The search criterion used targeted for the presence and frequency of any or all of the calcium-binding targets, i.e. (i) the EF-hand domain (Grzybowska 2018), (ii) the 9-residue RTX motif (GGXGXDXHX) (Grzybowska 2018) and (iii) the 17-residue calmodulin-binding sequence (e.g. KLWKKLLKLLKKLLKLG) (Kauer et al. 1986). As is shown in Fig. 3B, a single 16-residue calmodulin-binding sequence (IVQASVMAGIMKRRGR) was picked up between amino acids 251 and 268 and predicted to be the most likely binding site for Ca^{2+} in AtLHL (Yap et al. 2000). This outcome, besides strongly supporting our findings from the electrochemical analysis, also consistently and firmly corresponded with both the established binding properties and known key functions of AtLHL as an H1 family protein, whereby it is specifically responsible for binding to the nucleosome and linker DNA of the chromatin structure (Jeon and Berezney 1995).

Finally, after unequivocally establishing that AtLHL is a bona fide AC protein, we then went on to assess, determine and evaluate its reaction kinetics as an enzyme. As is seen in Fig. 3C, AtLHL was found to have a K_m constant of around 0.7 mM and a V_{max} constant of approximately 9.2 fmol/min/µg protein, comparable to other previously confirmed plant ACs. AtTIR1, AtAFB1 and AtAFB5 have K_m constants of 0.644, 0.602 and 0.675 mM and V_{max} constants of 7.462, 8.615 and 10.45 fmol/min/µg protein, respectively (Qi et al. 2022), while AtKUP7, AtClAP and MdTTM2 have V_{max} constants of 2.2, 7.3 and 8.3 fmol/min/µg protein, respectively (Al-Younis et al. 2015; Chatukuta et al. 2018; Yuan et al. 2022). Apparently, all plant ACs seem to have very low kinetics levels (high K_m and low V_{max} constants), suggesting that AC activity is not their main function but rather a secondary function as multi-functional or moonlighting proteins. The moonlight nature is typically exemplified in proteins such as AtKUP7, MpCAPE, AtNCED3, MdTTM1, AtDGK4 and AtTIR1, where AC activity is respectively combined with the permease, phosphodiesterase, dioxygenase, hydrolase, nitric oxide-binding and auxin perception activities (Al-Younis et al. 2015, 2021; Kasahara et al. 2016; Vaz Dias et al. 2019; Yuan et al. 2022; Qi et al. 2022). In AtTIR1, which is an auxin receptor, AC activity tightly controls auxin perception and ultimately the protein's main biological function of regulating root growth (Qi et al. 2022). This could be true for AtLHL, whereby the identified AC activity tightly controls its core functions, particularly those that it performs together with the other histone family proteins. This is not surprising because when we searched for presence of the AC centre in AtH2A, AtH2B, AtH3 and AtH4, none of these histone family proteins was found to possess the centre (results not shown).

Conclusion

In this study, we provide practical evidence that a linker histone-like or HNO4 protein from *Arabidopsis thaliana* (AtLHL) is a bona fide adenylyl cyclase (AC) capable of generating the second messenger, cAMP from ATP. AtLHL thus becomes the thirteenth AC to be identified in Arabidopsis and also the thirtieth AC identified in plants in general. Thus, considering that AtLHL appears to be the only histone family protein with AC activity and that it is typically involved in a number of key cellular processes such as chromatin formation (Jeon and Berezney 1995), embryogenesis (Martianov et al. 2005), reproduction (Tanaka et al. 2003), drought resistance (Ascenzi and Gantt 1997; Wu et al. 2022; Scippa et al. 2000) and disease resistance (Studencka et al. 2011), it is pertinent that more work is undertaken to perhaps shed more light onto its probable modes of action and at least functional significance in plants, particularly crops. Work involving the inactivation of its AC activity through site-directed mutations together with some in planta (in vivo) studies would be most ideal.

Author Contribution OR conceived the idea; OR and PC did the experiments. OR drafted the manuscript; and both authors read, edited, and approved the manuscript.

Funding Open access funding provided by North-West University. This work was funded by the North-West University (NWU) and the National Research Foundation (NRF) of South Africa (Grant Numbers: CSUR78843 & CSUR93635).

Availability of Data and Materials Not applicable.

Declarations

Ethical Approval Not applicable.

Competing Interests The authors declare no competing interests.

References

Albert I, Mavrich TN, Tomsho LP, Qi JL, Zanton SJ, Schuster SC, Franklin Pugh B (2007) Translational and rotational settings of H2A.Z nucleosomes across the *Saccharomyces cerevisiae* genome. Nature 446:572–576

Alberts B, Johnson A, Lewis J, Raff M, Roberts K, Walter P (2002) Chromosomal DNA and its packaging in the chromatin fiber. In: Molecular Biology of the Cell, 4th edn. Garland Science, New York

Al-Younis I, Moosa B, Kwiatkowski M, Jaworski K, Wong A, Gehring C (2021) Functional crypto-adenylate cyclases operate in complex plant proteins. Front Plant Sci 12:711749

Al-Younis I, Wong A, Gehring C (2015) The *Arabidopsis thaliana* K^+-uptake permease 7 (AtKUP7) contains a functional cytosolic adenylate cyclase catalytic centre. FEBS Lett 589(24PtB):3848–3852

Al-Younis I, Wong A, Lemtiri-Chlieh F, Schmöckel S, Tester M, Gehring C, Donaldson L (2018) The *Arabidopsis thaliana* K^+-uptake permease 5 (AtKUP5) contains a functional cytosolic adenylate cyclase essential for K^+ transport. Front Plant Sci 9:1645

Ascenzi R, Gantt JS (1997) A drought-stress-inducible histone gene in *Arabidopsis thaliana* is a member of a distinct class of plant linker histone variants. Plant Mol Biol 34:629–641

Bianchet C, Wong A, Quaglia M, Alqurashi M, Gehring C, Ntoukakis V, Pasqualini S (2019) An *Arabidopsis thaliana* leucine-rich repeat protein harbors an adenylyl cyclase catalytic center and affects responses to pathogens. J Plant Physiol 232:12–22

Blanco E, Fortunato S, Viggiano L, de Pinto MC (2020) Cyclic AMP: a polyhedral signalling molecule in plants. Int J Mol Sci 21(14):4862

Bobo ED, Sehlabane KS, Dikobe TB, Takundwa MM, Kawadza DT, Ruzvidzo O (2022) Identification and characterization of a soybean protein with adenylyl cyclase activity. Commun Plant Sci 12:50–59

Bonet-Costa C, Vilaseca M, Diema C, Vujatovic O, Vaquero A, Omeñaca N, Castejón L, Bernués J, Giralt E, Azorín F (2012) Combined bottom-up and top-down mass spectrometry analyses of the pattern of post-translational modifications of *Drosophila melanogaster* linker histone H1. J Proteom 75(13):4124–4138

Bradford MM (1976) A rapid and sensitive method for the quantitation of microgram quantities of protein utilizing the principle of protein-dye binding. Anal Biochem 72:248–254

Braun T, Dods RF (1975) Development of a Mn^{2+}-sensitive, "soluble" adenylate cyclase in rat testis. PNAS USA 72(3):1097–1101

Bustin M, Catez F, Lim JH (2005) The dynamics of histone H1 function in chromatin. Mol Cell 17(5):617–620

Calikowski T, Kozbial P, Kuras M, Jerzmanowski A (2000) Perturbation in linker histone content has no effect on the cell cycle but affects the cell size of suspension grown tobacco BY-2 cells. Plant Sci 157(1):51–63

Chatukuta P, Dikobe TB, Kawadza DT, Sehlabane KS, Takundwa MM, Wong A, Gehring C, Ruzvidzo O (2018) An Arabidopsis clathrin assembly protein with a predicted role in plant defense can function as an adenylate cyclase. Biomolecules 8(2):15

Chen J, Kinyamu HK, Archer TK (2006) Changes in attitude, changes in latitude: nuclear receptors remodeling chromatin to regulate transcription. Mol Endocrinol 20(1):1–13

Chen Y, Cann MJ, Litvin TN, Iourgenko V, Sinclair ML, Levin LR, Buck J (2000) Soluble adenylyl cyclase as an evolutionarily conserved bicarbonate sensor. Science 289(5479):625–628

Davey CA, Sargent DF, Luger K, Maeder AW, Richmond TJ (2002) Solvent mediated interactions in the structure of the nucleosome core particle at 1.9 a resolution. J Mol Biol 319(5):1097–1113

Dekker J (2008) Mapping in vivo chromatin interactions in yeast suggests an extended chromatin fiber with regional variation in compaction. J Biol Chem 283(50):34532–34540

Deterding LJ, Bunger MK, Banks GC, Tomer KB, Archer TK (2008) Global changes in and characterization of specific sites of phosphorylation in mouse and human histone H1 isoforms upon CDK inhibitor treatment using mass spectrometry. J Proteome Res 7(6):2368–2379

Duszyn M, Świeżawska-Boniecka B, Skorupa M, Jaworski K, Szmidt-Jaworska A (2022) BdGUCD1 and cyclic GMP are required for responses of *Brachypodium distachyon* to *Fusarium pseudograminearum* in the mechanism involving jasmonate. Int J Mol Sci 23(5):2674

Ehsan H, Reichheld JP, Roef L, Witters E, Lardon F, Van Bockstaele D, Van Montagu M, Inzé D, Van Onckelen H (1998) Effect of indomethacin on cell cycle dependent cyclic AMP fluxes in tobacco BY-2 cells. FEBS Lett 422(2):165–169

Garcia BA, Busby SA, Barber CM, Shabanowitz J, Allis CD, Hunt DF (2004) Characterization of phosphorylation sites on histone H1 isoforms by tandem mass spectrometry. J Proteome Res 3(6):1219–1227

Gastreich M, Lilienthal M, Briem H, Claussen H (2006) Ultrafast de novo docking combining pharmacophores and combinatorics. J Comput Aided Mol Des 20(12):717–734

Gehring C (2010) Adenyl cyclases and cAMP in plant signaling - past and present. Cell Commun Signal 8:15

Gerisch G, Hülser D, Malchow D, Wick U (1975) Cell communication by periodic cyclic-AMP pulses. Biol Sci 272(915):181–192

Goodman DB, Rasmussen H, DiBella F, Guthrow CE (1970) Cyclic adenosine 3':5'-monophosphate-stimulated phosphorylation of isolated neurotubule subunits. Proc Natl Acad Sci USA 67(2):652–659

Grzybowska EA (2018) Calcium-binding proteins with disordered structure and their role in secretion, storage, and cellular signaling. Biomolecules 8:42

Harshman SW, Young NL, Parthun MR, Freitas MA (2013) H1 histones: current perspectives and challenges. Nucleic Acids Res 41(21):9593–9609

Hergeth SP, Schneider R (2015) The H1 linker histones: multifunctional proteins beyond the nucleosomal core particle. EMBO Rep 16(11):1439–1453

Irving HR, Kwezi L, Wheeler J, Gehring C (2012) Moonlighting kinases with guanylate cyclase activity can tune regulatory signal networks. Plant Signal Behav 7:201–204

Ito M, Takahashi H, Sawasaki T, Ohnishi K, Hikichi Y, Kiba A (2014) Novel type of adenylyl cyclase participates in tabtoxinine-β-lactam-induced cell death and occurrence of wildfire disease in *Nicotiana benthamiana*. Plant Signal Behav 9(1):e27420

Jeon KW, Berezney R (1995) Structural and functional organization of the nuclear matrix. Academic Press, Boston, pp 214–217

Jiang T, Zhou X, Taghizadeh K, Dong M, Dedon PC (2007) N-formylation of lysine in histone proteins as a secondary modification arising from oxidative DNA damage. Proc Natl Acad Sci USA 104(1):60–65

Jin XC, Wu WH (1999) Involvement of cyclic AMP in ABA- and Ca^{2+}-mediated signal transduction of stomatal regulation in *Vicia faba*. Plant Cell Physiol 40:1127–1133

Kamenetsky M, Middelhaufe S, Bank EM, Levin LR, Buck J, Steegborn C (2006) Molecular details of cAMP generation in mammalian cells: a tale of two systems. J Mol Biol 362(4):623–639

Kasahara M, Suetsugu N, Urano Y, Yamamoto C, Ohmori M, Takada Y, Okuda S, Nishiyama T, Sakayama H, Kohchi T, Takahashi F (2016) An adenylyl cyclase with a phosphodiesterase domain in basal plants with a motile sperm system. Sci Rep 6:39232

Katoh K, Rozewicki J, Kazunori D, Yamada KD (2019) MAFFT online service: multiple sequence alignment, interactive sequence choice and visualization. Brief Bioinform 20(4):1160–1166

Kauer JC, Erickson-Viitanen S, Wolfe HR, DeGrado WF (1986) Photolabeling of calmodulin with a synthetic calmodulin-binding peptide. J Biol Chem 261(23):10695–10700

Kawadza D, Dikobe T, Chatukuta P, Takundwa M, Bobo E, Sehlabane K, Ruzvidzo O (2022) An Arabidopsis maternal effect embryo arrest protein is an adenylyl cyclase with predicted roles in embryo development and response to abiotic stress. TOBIOTJ 16(1)

Kim JM, Kim K, Punj V, Liang G, Ulmer TS, Lu W, An W (2015) Linker histone H1.2 establishes chromatin compaction and gene silencing through recognition of H3K27me3. Sci Rep 5:16714

Kim K, Jeong KW, Kim H, Choi J, Lu W, Stallcup MR, An W (2012) Functional interplay between p53 acetylation and H1.2 phosphorylation in p53-regulated transcription. Oncogene 31(39):4290–4301

Liu Z, Yuan Y, Wang L (2023) Three novel adenylate cyclase genes show significant biological functions in plant. J Agric Food Chem 71(2):1149–1161

Lu X, Wontakal SN, Emelyanov AV, Morcillo P, Konev AY, Fyodorov DV, Skoultchi AI (2009) Linker histone H1 is essential for Drosophila development, the establishment of pericentric heterochromatin, and a normal polytene chromosome structure. Genes Dev 23(4):452–465

Ludidi N, Gehring C (2003) Identification of a novel protein with guanylyl cyclase activity in *Arabidopsis thaliana*. J Biol Chem 278(8):6490–6494

Luger K, Mäder AW, Richmond RK, Sargent DF, Richmond TJ (1997) Crystal structure of the nucleosome core particle at 2.8 A resolution. Nature 389(6648):251–260

Ma W, Qi Z, Smigel A, Walker RK, Verma R, Berkowitz GA (2009) Ca^{2+}, cAMP, and transduction of non-self-perception during plant immune responses. Proc Natl Acad Sci USA 106(49):20995–21000

Malho R, Camacho L, Moutinho A (2000) Signalling pathways in pollen tube growth and reorientation. Ann Bot 85:59–68

Martianov I, Brancorsini S, Catena R, Gansmuller A, Kotaja N, Parvinen M, Sassone-Corsi P, Davidson I (2005) Polar nuclear localization of H1T2, a histone H1 variant, required for spermatid elongation and DNA condensation during spermiogenesis. Proc Natl Acad Sci USA 102(8):2808–2813

Misteli T, Gunjan A, Hock R, Bustin M, Brown DT (2000) Dynamic binding of histone H1 to chromatin in living cells. Nature 408(6814):877–881

Moutinho A, Hussey PJ, Trewavas AJ, Malhó R (2001) cAMP acts as a second messenger in pollen tube growth and reorientation. Proc Natl Acad Sci USA 98(18):10481–10486

Mulaudzi T, Ludidi N, Ruzvidzo O, Morse M, Hendricks N, Iwuoha E, Gehring C (2011) Identification of a novel *Arabidopsis thaliana* nitric oxide-binding molecule with guanylate cyclase activity in vitro. FEBS Lett 585(17):2693–2697

Naumova N, Imakaev M, Fudenberg G, Zhan Y, Lajoie BR, Mirny LA, Dekker J (2013) Organization of the mitotic chromosome. Science 342(6161):948–953

Parseghian MH, Henschen AH, Krieglstein KG, Hamkalo BA (1994) A proposal for a coherent mammalian histone H1 nomenclature correlated with amino acid sequences. Protein Sci 3(4):575–587

Pettersen EF, Goddard TD, Huang CC, Meng EC, Couch GS, Croll TI, Morris JH, Ferrin TE (2021) UCSF ChimeraX: structure visualization for researchers, educators, and developers. Protein Sci 30(1):70–82

Poirier GG, de Murcia G, Jongstra-Bilen J, Niedergang C, Mandel P (1982) Poly(ADP-ribosyl)ation of polynucleosomes causes relaxation of chromatin structure. Proc Natl Acad Sci USA 79(11):3423–3427

Qi L, Kwiatkowski M, Chen H, Hoermayer L, Sinclair S, Zou M, del Genio CI, Kubeš MF, Napier R, Jaworski K, Friml J (2022) Adenylate cyclase activity of TIR1/AFB auxin receptors in plants. Nature 611:133–137

Robison GA, Butcher RW, Sutherland EW (1968) Cyclic AMP. Annu Rev Biochem 37:149–174

Roelofs J, Meima M, Schaap P, Van Haastert PJ (2001) The Dictyostelium homologue of mammalian soluble adenylyl cyclase encodes a guanylyl cyclase. EMBO J 20(16):4341–4348

Ruzvidzo O, Dikobe BT, Kawadza DT, Mabadahanye GH, Chatukuta P, Kwezi L (2013) Recombinant expression and functional testing of candidate adenylate cyclase domains. Methods Mol Biol 1016:13–25

Ruzvidzo O, Gehring C, Wong A (2019) New perspectives on plant adenylyl cyclases. Front Mol Biosci 6:136

Sabetta W, Vandelle E, Locato V, Costa A, Cimini S, Bittencourt Mour A, Luoni L, Graf A, Viggiano L, De Gara L, Bellin D, Blanco E, de Pinto MC (2019) Genetic buffering of cyclic AMP in *Arabidopsis thaliana* compromises the plant immune response triggered by an avirulent strain of *Pseudomonas syringae* pv. tomato. Plant J 98(4):590–606

Sarg B, Lopez R, Lindner H, Ponte I, Suau P, Roque A (2015) Identification of novel post-translational modifications in linker histones from chicken erythrocytes. J Proteom 113:162–177

Scippa GS, Griffiths A, Chiatante D, Bray EA (2000) The H1 histone variant of tomato, H1-S, is targeted to the nucleus and accumulates in chromatin in response to water-deficit stress. Planta 211(2):173–181

Sehlabane K, Chatukuta P, Dikobe T, Bobo E, Sibanda A, Kawadza D, Ruzvidzo O (2022) A putative protein with no known function in *Arabidopsis thaliana* harbors a domain with adenylyl cyclase activity. Am J Plant Sci 13:943–959

Shah S, Peterkofsky A (1991) Characterization and generation of *Escherichia coli* adenylate cyclase deletion mutants. J Bacteriol 173(10):3238–3242

Snijders AP, Pongdam S, Lambert SJ, Wood CM, Baldwin JP, Dickman MJ (2008) Characterization of post-translational modifications of the linker histones H1 and H5 from chicken erythrocytes using mass spectrometry. J Proteome Res 7(10):4326–4335

Steer ML, Levitzki A (1975) The control of adenylate cyclase by calcium in turkey erythrocyte ghosts. J Biol Chem 250(6):2080–2084

Studencka M, Konzer A, Moneron G, Wenzel D, Opitz L, Salinas-Riester G, Bedet C, Kruger M, Hell SW, Wisniewski JR, Schmidt H, Palladino F, Schulze E, Jedrusik-Bode M (2011) Novel roles of *Caenorhabditis elegans* heterochromatin protein HP1 and linker histone in the regulation of innate immune gene expression. Mol Cell Biol 32:251–265

Swieżawska B, Jaworski K, Pawełek A, Grzegorzewska W, Szewczuk P, Szmidt-Jaworska A (2014) Molecular cloning and characterization of a novel adenylyl cyclase gene, HpAC1, involved in stress signaling in *Hippeastrum hybridum*. Plant Physiol Biochem 80:41–52

Świeżawska B, Duszyn M, Kwiatkowski M, Jaworski K, Pawełek A, Szmidt-Jaworska A (2020) *Brachypodium distachyon* triphosphate tunnel metalloenzyme 3 is both a triphosphatase and an adenylyl cyclase upregulated by mechanical wounding. FEBS Lett 594(6):1101–1111

Tanaka M, Kihara M, Meczekalski B, King GJ, Adashi EY (2003) H1oo: a pre-embryonic H1 linker histone in search of a function. Mol Cell Endocrinol 202:5–9

Tezuka T, Hiratsuka S, Takahashi SY (1993) Promotion of the growth of self-incompatible pollen tubes in lily by cAMP. Plant Cell Physiol 34(6):955–958

Thoma F, Koller T (1977) Influence of histone H1 on chromatin structure. Cell 12(1):101–107

Thoma F, Koller T, Klug A (1979) "Involvement of histone H1 in the organization of the nucleosome and of the salt-dependent superstructures of chromatin." J Cell Biol 83(2Pt1):403–427

Trott O, Olson AJ (2010) AutoDock Vina: improving the speed and accuracy of docking with a new scoring function, efficient optimization, and multithreading. J Comput Chem 31(2):455–461

Tucker CL, Hurley JH, Miller TR, Hurley JB (1998) Two amino acid substitutions convert a guanylyl cyclase, RetGC-1, into an adenylyl cyclase. Proc Natl Acad Sci USA 95(11):5993–5997

Ullmann A, Danchin A (1983) Role of cyclic AMP in bacteria. Adv Cyclic Nucleotide Res 15:1–53

van Holde K, Zlatanova J (1996) What determines the folding of the chromatin fiber? Proc Natl Acad Sci USA 93(20):10548–10555

Varadi M, Anyango S, Deshpande M, Nair S, Natassia C, Yordanova G, Yuan D, Stroe O, Wood G, Laydon A, Žídek A, Green T, Tunyasuvunakool K, Petersen S, Jumper J, Clancy E, Green R, Vora A, Lutfi M, Figurnov M, Velankar S (2022) AlphaFold protein structure database: massively expanding the structural coverage of protein-sequence space with high-accuracy models. Nucleic Acids Res 50(D1):D439–D444

Vaz Dias F, Serrazina S, Vitorino M, Marchese D, Heilmann I, Godinho M, Rodrigues M, Malhó R (2019) A role for diacylglycerol kinase 4 in signalling crosstalk during Arabidopsis pollen tube growth. New Phytol 222(3):1434–1446

Villar-Garea A, Imhof A (2006) The analysis of histone modifications. Biochim Biophis Acta 1764(12):1932–1939

Wisniewski JR, Zougman A, Krüger S, Mann M (2007) Mass spectrometric mapping of linker histone H1 variants reveals multiple acetylations, methylations, and phosphorylation as well as differences between cell culture and tissue. Mol Cell Proteom 6(1):72–87

Wisniewski JR, Zougman A, Mann M (2008) Nepsilon-formylation of lysine is a widespread post-translational modification of nuclear proteins occurring at residues involved in regulation of chromatin function. Nucleic Acids Res 36(2):570–577

Wu X, Xu J, Meng X, Fang X, Xia M, Zhang J, Cao S, Fan T (2022) Linker histone variant HIS1-3 and WRKY1 oppositely regulate salt stress tolerance in Arabidopsis. Plant Physiol 189(3):1833–1847

Xiao B, Freedman BS, Miller KE, Heald R, Marko JF (2012) Histone H1 compacts DNA under force and during chromatin assembly. Mol Biol Cell 23(24):4864–4871

Xu N, Zhang C, Lim LL, Wong A (2018) Bioinformatic analysis of nucleotide cyclase functional centers and development of ACPred webserver. In: Proceedings of the 2018 ACM International Conference on Bioinformatics, Computational Biology, and Health Informatics (BCB '18), New York, NY: Association for Computing Machinery, 122–129

Yang H, Zhao Y, Chen N, Liu Y, Yang S, Du H, Wang W, Wu J, Tai F, Chen F, Hu X (2021) A new adenylyl cyclase, putative disease-resistance RPP13-like protein 3, participates in abscisic acid-mediated resistance to heat stress in maize. J Exp Bot 72(2):283–301

Yap KL, Kim J, Truong K, Sherman M, Yuan T, Ikura M (2000) Calmodulin target database. J Struct Funct 1(1):8–14

Yuan Y, Liu Z, Wang L, Wang L, Chen S, Niu Y, Zhao X, Liu P, Liu M (2022) Two triphosphate tunnel metalloenzymes from apple exhibit adenylyl cyclase activity. Front Plant Sci 13:992488

Zhang Y (2008) I-TASSER server for protein 3D structure prediction. BMC Bioinform 9:40

Zhou W, Chi W, Shen W, Dou W, Wang J, Tian X, Gehring C, Wong A (2021) Computational identification of functional centers in complex proteins: a step-by-step guide with examples. Front Bioinform 1:652286

Authors and Affiliations

Oziniel Ruzvidzo[1] · Patience Chatukuta[1]

✉ Oziniel Ruzvidzo
Oziniel.Ruzvidzo@nwu.ac.za

[1] Department of Botany, School of Biological Sciences, North-West University, Private Bag X2046, Mmabatho 2735, South Africa